JOURNAL OF OPTOELECTRONICS AND ADVANCED MATERIALS Vol. 10, No. 8, August 2008, p. 2117 - 2122

Raman studies and optical properties of lead-bismuth metaborate glasses

H. TICHA*, K. KNOBLOCHOVA, L.TICHY[a]
Faculty of Chemical Technology, University of Pardubice, 532 10 Pardubice, Czech Republic
[a]Joint Laboratory of Solid State Chemistry of Institute of Macromolecular Chemistry of the Academy of Sciences of the Czech Republic and University of Pardubice, 532 10 Pardubice, Czech Republic

Four $(PbO)_x(Bi_2O_3)_{0.5-x}(B_2O_3)_{0.5}$ metaborate glasses, where x = 0.1, 0.2, 0.3 and 0.4 were prepared. The dilatometric glass-transition temperature was found to be practically invariant to x, while both the density and the molar volume increased with substitution of PbO by Bi_2O_3. Raman spectra indicated that substitution of PbO by Bi_2O_3 shifted most probably the dynamical equilibrium between metaborate triangles and tetrahedra in direction of metaborate triangles formation. An increase in the Bi_2O_3 content enhanced relative intensity of the Raman scattering for the wavenumbers from 200 to 500 cm^{-1}. The optical gap (E_g) was found in the region 3.41 (x = 0.1) < E_g [eV] < 3.63 (x = 0.4) and the coefficient of its temperature dependence (γ, [eV/K]) varied from 5.35×10^{-4} to 5.91×10^{-4}. The non-linear refractive index (n_2, [esu]) estimated from the optical gap values was found slightly increasing with Bi_2O_3 content from 5.35×10^{-11} to 5.91×10^{-11}.

(Received April 4, 2008; accepted June 30, 2008)

Keywords: Borate glasses, Raman spectroscopy, optical properties

1. Introduction

Among heavy metal oxide glasses (HMOG) the glasses of $PbO\text{-}Bi_2O_3\text{-}B_2O_3$ system have shown a promise for broad potential applications in optical devices, where their interesting optical properties sufficiently wide optical gap, high linear and non-linear refractive index, appropriate thermal stability [1] and a resistance to water corrosion, are utilized. Due to small multi-phonon relaxations, $PbO\text{-}Bi_2O_3\text{-}B_2O_3$ glasses are interesting as host materials for rare-earth doping to get efficient fluorescence emissions [2, 3]. High content of heavy metals makes these glasses interesting in relation to an influence of γ- ray on their optical and structural properties, for instance the effect of the gamma-irradiation shielding [4]. Recently we have studied (i) role of substitution of B_2O_3 by PbO on structural make-up of $(PbO)_x(Bi_2O_3)_{0.2}(B_2O_3)_{0.8-x}$ glasses by Raman spectroscopy and (ii) various physical properties inclusive optical properties in the region of the short wavelength absorption edge [5].

In the present paper our attention is given to the role of substitution of PbO by Bi_2O_3 on the structural arrangement and on the optical properties of metaborate $(PbO)_x(Bi_2O_3)_{0.5-x}(B_2O_3)_{0.5}$ glasses. An attempt is given to correlate qualitatively the results of Raman spectroscopy with the changes observed in the short wavelength absorption edge.

2. Experimental

The glasses studied were prepared in batches of 20 g from PbO, Bi_2O_3, and B_2O_3 (purity better than 98 %, supplied by Sigma Aldrich) homogenized and melted in a covered platinum crucible in an electrical furnace at the temperature (T) around 830 °C for 1 hour. The melt was frequently homogenized by swirling of the crucible and a homogeneous glass-forming liquid was poured onto a stainless plate at the room temperature. Well transparent yellowish glassy samples (confirmed by an absence of X-ray diffraction patterns) were obtained.

The chemical composition of glasses was verified using microprobe X-ray analysis (JEOL JSM 5500 LV, accuracy ± 1.5 at % of an element).

The density (ρ) was determined at room temperature following Archimedean principle; the CCl_4 was used as the immersion medium. With respect to the error in the density determination the molar volume values, $V_M = M/\rho$ (M is the average molar weight) are accurate to within ± 0.05 cm^3/mol.

The glass transition temperature (T_g) and "dilatometric" glass temperature (T_d) were obtained by means of thermo-mechanical analysis (TMA) using the tangents intersection technique (T_g) and as an extreme (T_d) on the dependence of the sample expansion on the temperature. The heating rate of the samples (the glass cube $0.5\times0.5\times0.5$ cm^3) was 5 °C/min, load ≈ 10 mN (TMAnalyzer CX04, Czech Republic). The accuracy of both T_g and T_d values was found at around ± 3 °C.

Raman spectra were recorded on an FTIR spectrometer, Bruker model IFS 55 with Raman attachment FRA 106, in backscattering geometry using a Nd:YAG laser radiation (excitation light wavelength 1064 nm, a slit width of 4 cm^{-1}, the laser power ≈ 300 mW at the sample surface). Raman spectra were measured at room temperature in the spectral region 50 - 1500 cm^{-1} using 200 scans on the bulk sample.

Optical transmission in UV-VIS spectral region was measured on the samples prepared by a glass blowing method. The samples with the thickness (d) varying in the region $3 \le d[\mu m] \le 6$, were used. Optical transmission of

all prepared glasses was measured, in the temperature interval 300 - 600 K, using an optical thermostat O.T.I. (R.M.I., Czech Republic) placed in the HP 8453 spectrophotometer. Assuming non-direct optical transitions, the optical gap values ($E_{g,non}$), for the samples x = 0.1, 0.2, 0.3 and 0.4, were determined from the relation [6]: $(Kh\nu)^{1/2} = B^{1/2}(h\nu - E_{g,non})$, where $B^{1/2}$, the slope of the short wavelength absorption edge (SWAE), reflects the sample disorder [6], hν is the photon energy, and K, the absorption coefficient, is calculated using the relation $K = (1/d)\ln\{[(1 - R)^2 + ((1 - R)^4 + 4R^2T^2)^{1/2}]/2T\}$, where R is the reflectance and T is the transmission, respectively. The values of R ≈ 0.1; 0.095; 0.09 and 0.09 for x = 0.1, 0.2, 0.3 and 0.4, respectively, invariant to the wavelength within a narrow spectral region of SWAE, were used to determine K values. Refractive index (n) values ($n = 1/T + (1/T^2 - 1)^{1/2}$) were estimated from the optical transmission in transparent window at the wavelength λ = 800 nm.

3. Results

In Fig. 1 typical spectral dependencies of the optical transmission for the sample (x = 0.3) prepared by glass blowing are shown. In the inset the SWAE is shown in $(Kh\nu)^{1/2}$ versus hν coordinates. The temperature dependence of the optical gap is shown in Fig. 2. The chemical composition of glasses studied, their density (ρ), the molar volume (V_M), both the glass-transition (T_g) and softening (T_d) temperatures, the optical gap (E_g) and the refractive index values are summarized in Table 1. Our experimental values of T_g seem to be in harmony with T_g values reported for similar glasses: T_g(x = 0.5) = 389 °C, [7], T_g(x = 0) = 360 °C, [8] and T_g(x = 0.25) = 387 °C, [9], respectively. Our refractive index (n) values also correspond to n values of relevant binary glasses: n(x = 0.5) = 1.87, [10], and n(x = 0) = 2.09, [11], respectively. The value for n(x = 0) we calculated

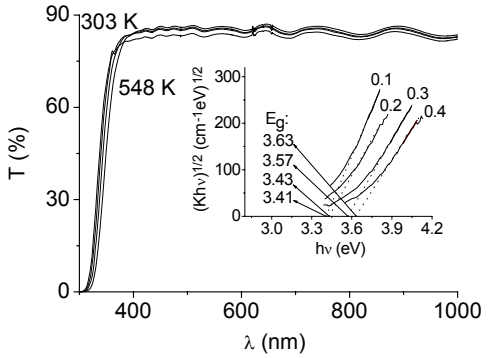

Fig. 1. Spectral dependencies of the optical transmission of $(Bi_2O_3)_{0.2}(PbO)_{0.3}(B_2O_3)_{0.5}$ sample measured in the temperature interval from 303 to 548 K. In the inset the spectral dependencies of the short wavelength absorption edge (T ≈ 300 K) for all glasses assuming non-direct optical transitions is displayed.

from eq. 4 and relevant data in Table 1 in [11]. The optical gap values correspond quite well to the compositional trend in E_g(x) values inferred from the data in Fig. 5 in [12].

Table 1. Chemical composition expressed as the molar fraction of PbO (x), density (ρ, g/cm^3), molar volume ($V_{M,E}$, cm^3/mol), dilatometric glass transition (T_g, ºC)/glass softening (T_d, ºC) temperature, the values of the optical gap (E_g, eV) and the values of linear refractive index (n) of the glasses studied.

x	ρ	$V_{M,E}$	T_g/ T_d	E_g	n
0.1	6.85	35.57	393/ 426	3.41	1.99
0.2	6.64	33.02	393/ 422	3.43	1.89
0.3	6.41	30.41	393/ 427	3.57	1.88
0.4	6.13	27.84	391/ 425	3.63	1.87

Following facts are evident from Table 1 and Figs. 1 and 2: (i) the substitution of PbO by Bi_2O_3 leads to an increase in both the density and the molar volume, analogously to the results in [13]; (ii) the glass-transition temperature is practically invariant to the chemical composition. The relative independence of T_g on the ratio of PbO and Bi_2O_3 in borate glasses has been noted also in [14]; (iii) the optical gap increases with an increase in PbO content.

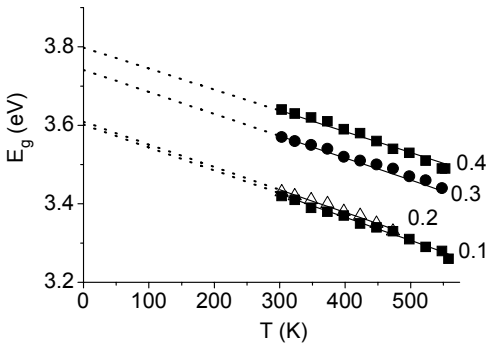

Fig. 2. Temperature dependencies of the optical gap ($E_g(T)$) for the studied $(PbO)_x(Bi_2O_3)_{0.5-x}(B_2O_3)_{0.5}$ glasses. The points - experimental data, the dotted lines - the linear extrapolation ($E_g(T) = E_g(0) - \gamma T$), see Table 2), the numbers indicate the chemical composition, see Table 1.

In Fig. 3 overall Raman spectra in the wavenumber region 100 - 1500 cm^{-1} are shown. An attempt to decompose the spectra into individual bands did not give satisfactory results. We have obtained at least 14 bands and the quality of decomposition is only weakly sensitive

to the number of bands used for the experimental spectra fitting. In such case, the decomposition has rather problematical physical significance.

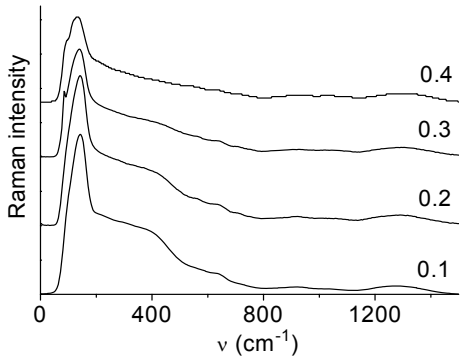

Fig. 3. Overall Raman spectra of $(PbO)_x(Bi_2O_3)_{0.5-x}(B_2O_3)_{0.5}$ glasses. The numbers indicate the chemical composition, see Table 1.

Hence, following our recent communication [5], we have decomposed the two most typical parts of Raman spectra, namely the wavenumber region 100 - 600 cm^{-1}, where dominant role is played by vibrational modes associated with the presence of heavy metal atom (HMA)-oxygen bonds, and the region 700 - 1500 cm^{-1} where vibrational modes associated mainly with borate network are important. For the most interesting glasses with the chemical composition x = 0.1 and x = 0.4 the decomposed spectra are shown in Fig. 4 a, b. Raman features (RF) in the region 70 - 160 cm^{-1}, Fig. 4 a, correspond mainly to heavy metal ion vibration, RF in 300 - 600 cm^{-1} region correspond mainly to symmetrically bridged anion modes of the type $(HMA)_1$-O-$(HMA)_1$ [15, 16] and to asymmetrically bridged anion modes of type $(HMA)_2$-O-$(HMA)_1$, namely close to 600 cm^{-1} [17].

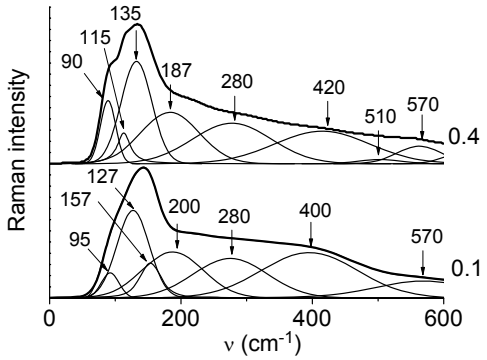

Fig. 4a. Decomposed Raman spectra of glasses with x = 0.1 and x = 0.4, in the wavenumber region of 100 - 600 cm^{-1}. The spectrum for x = 0.4 is multiplied by twice for better resolution, for details, see text.

The Raman features in Fig. 4 b, the region 700 - 1500 cm^{-1}, correspond to some typical RF of borate network namely: RF(ν > 1100 cm^{-1}) to B - O stretching modes of triangular (BO_3) arrangement, RF(ν < 800 cm^{-1}) to bending modes in BO_3 units, and the stretching modes in tetrahedral (BO_4) arrangement: RF($\nu_1 \approx$ 700 - 760 cm^{-1}), RF($\nu_2 \approx$ 500 - 550 cm^{-1}), RF($\nu_3 \approx$ 900 and 1000 cm^{-1}) [18, 19], respectively.

4. Discussion

4.1. Structural consideration

In Fig. 3 some Raman scattering changes are seen, namely an increase in Raman intensity in the region 200 - 600 cm^{-1} with a decrease in x that is with substitution of PbO by Bi_2O_3. The bond energy (E_B) of Bi - O and Pb - O bonds is similar: E_B(Bi - O) ≈ 24.5 Kcal/A.b. and E_B(Pb - O) ≈ 24.2 Kcal/A.b., (A.b. is Avogadro´s bond) [20]; the bond distance (a) of Bi - O and Pb - O bonds is similar:a(Bi - O) ≈ 2.4 Å, a(Pb - O) ≈ 2.5Å [21], and the atomic mass of Bi and Pb atoms is nearly the same (208.98 for Bi and 207.19 for Pb), respectively. Hence, in the first approximation the stretching force constant for Bi - O and Pb - O should be very similar and observed changes in Raman scattering intensity we attribute mainly to an increase in the number of HMA - O bonds. A substitution of one mole of PbO by one mole of Bi_2O_3 means that one Pb atom is substituted by two Bi atoms and, simultaneously, the molar fraction O/HMA increases from 1 for PbO to 1.5 for Bi_2O_3.

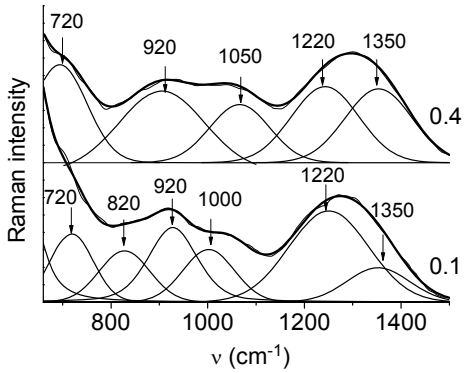

Fig. 4b. Decomposed Raman spectra of glasses with x = 0.1 and x = 0.4, in the wavenumber region of 700 - 1500 cm^{-1}. For details, see text.

Explicitly, for x = 0.1, the total number of HMA/cm^3 is around 1.52×10^{22} atoms/cm^3, whereas for x = 0.4 it is 1.29×10^{22} atoms/cm^3.

In Fig. 4a, Raman envelope in the region 100 - 600 cm^{-1} is decomposed into Raman features which we, following relevant literature, have attributed as follows:

(i) x = 0.4: RF($\nu \approx 90$ cm^{-1}), RF($\nu \approx 115$ cm^{-1}), RF($\nu \approx 135$ cm^{-1}), and RF($\nu \approx 187$ cm^{-1}) to "heavy metal modes" [22] and RF($\nu \approx 280$ cm^{-1}), RF($\nu \approx 420$ cm^{-1}) and RF($\nu \approx 510, 570$ cm^{-1}) to symmetric stretching oxygen motion in Pb-O-Pb bridge but also in asymmetric Pb-O-Bi bridge [22]. The presence of well resolved RF at around 90 cm^{-1}, 140 cm^{-1}, 280 cm^{-1} indicates similar structural arrangement around the lead atoms as in β-PbO exists with lead atom at the apex of PbO_4 pyramid [23].

(ii) x = 0.1: RF($\nu \approx 95$ cm^{-1}), RF($\nu \approx 127$ cm^{-1}) and RF($\nu \approx 157$ cm^{-1}) to "heavy metal modes"[22] more specifically RF($\nu \approx 127$ cm^{-1}) and RF($\nu \approx 157$ cm^{-1}) indicate presence of Bi^{3+} in [BiO_6] octahedral units [16], RF($\nu \approx 200$ cm^{-1}), RF($\nu \approx 280$ cm^{-1}), RF($\nu \approx 400$ cm^{-1}) and RF($\nu \approx 570$ cm^{-1}), respectively, to symmetric stretching oxygen motion in angularly constrained bridge, namely Bi-O-Bi in [BiO_6] polyhedra [24, 25]. Some broadening of these RF could be associated with disorder since, in fact three types of bridges (Bi-O-Bi, Pb-O-Bi, Pb-O-Pb) might coexist in studied glasses and, in addition, [BiO_6] polyhedra are most probably strongly deformed.

In relation to borate network, studied $(PbO)_x(Bi_2O_3)_{0.5-x}(B_2O_3)_{0.5}$ glasses belong to the family of glasses where local structural arrangement can be described by some dynamical equilibrium between metaborate triangles ($B\emptyset_2O^-$) and tetrahedra ($B\emptyset_4^-$): $B\emptyset_2O^- \leftrightarrow B\emptyset_4^-$, [26], where Ø is the bridging oxygen. Decomposition of Raman envelope in the wavenumber region 700 - 1500 cm^{-1} is shown in Fig. 4b for the samples x = 0.4 and x = 0.1. Decomposed Raman features can be attributed as follows:

(i) x = 0.4: RF($\nu \approx 720$ cm^{-1}) to chain of metaborate [27], the broad RF($\nu \approx 920$ cm^{-1}) to $B\emptyset_4^-$, RF($\nu \approx 1050$ cm^{-1}) to structural arrangement where both metaborate triangles and tetrahedra are involved, RF($\nu \approx 1220$ cm^{-1}) to stretching mode of triangular unit and RF($\nu \approx 1350$ cm^{-1}) to terminal B-O$^-$ bonds in $B\emptyset_2O^-$, [26];

(ii) x = 0.1: RF($\nu \approx 720$ cm^{-1}) similarly as for x = 0.4 belongs to chain of metaborate. New RF at around 820 cm^{-1} appeared and RF($\nu \approx 920$ cm^{-1}) is significantly narrowed in comparison to RF($\nu \approx 920$ cm^{-1}) for x = 0.4. This is an indication that substitution of PbO by Bi_2O_3 leads to some ordering at least around $B\emptyset_4^-$ tetrahedra and their density probably decreases. Simultaneously, relative intensity of RF ($\nu \approx 1220$ cm^{-1}) increases which might indicate an increase in the density of triangular units. This observation implies some shift of the equilibrium $B\emptyset_2O^- \leftrightarrow B\emptyset_4^-$ on the left hand side. A decrease in relative intensity of RF ($\nu \approx 1350$ cm^{-1}) indicates a decrease in the density of terminal B-O$^-$ bonds in $B\emptyset_2O^-$ triangles. Hence, we suggest that the substitution of Bi_2O_3 by PbO results to an increase in structural order of borate network. It is also indicated by new RF (≈ 820 cm^{-1}), which could be attributed to the symmetric stretching of the B-O-B bridging bonds [28].

Rather subtle changes in Raman scattering of studied metaborate glasses suggest that the substitution of Bi_2O_3 by PbO results to an enhancement in relative intensity of Raman scattering, namely in the wavenumber region 200 - 600 cm^{-1}, which we associate with an increase in the density of HMA-O-HMA bridges. Simultaneously, the substitution of PbO by Bi_2O_3 results in some ordering in borate network indicated by considerable narrowing in RF($\nu \approx 920$ cm^{-1}) attributed to $B\emptyset_4^-$ tetrahedral units. These rather subtle structural changes are not reflected in the glass-transition temperature, which - together with the softening temperature - is practically invariant to the chemical composition (see Table 1).

The fact that in the examined glasses the metaborate network dominates is supported by calculation of the molar volume ($V_{M,C}$). Using the simple additive model: $V_{M,C} = \sum x_i V_{Mi}$, x_i and V_{Mi} are molar fraction and molar volume of PbO, Bi_2O_3 and B_2O_3, respectively, the agreement between experimental and calculated molar volume values can not be obtained for reasonable V_{Mi} values. It is easy to show that for $(PbO)_x(B_2O_3)_{1-x}$(I) and $(Bi_2O_3)_x(B_2O_3)_{1-x}$(II) glassy systems the molar volume could be calculated using the relation:

$V_{M,C}$ (I) = $xV_{M,PbO} + (1 - x)V_{M,B2O3} - \gamma_I x(1 - x)$, and $V_{M,C}$ (II) = $xV_{M,Bi2O3} + (1 - x)V_{M,B2O3} - \gamma_{II} x(1 - x)$. Using the data $V_M(x)$ for both (I, II) binary systems [29] good fit $V_{M,C}$(I) and $V_{M,C}$(II) to experimental V_M data we have obtained for $V_{M,PbO}$ = 26.26 cm^3/mol, $V_{M,Bi2O3}$ = 52.36 cm^3/mol, $V_{M,\ B2O3}$ = 38.75 cm^3/mol and γ_I = 34 cm^3/mol and γ_{II} = 32 cm^3/mol. For our $(PbO)_x(Bi_2O_3)_{0.5-x}(B_2O_3)_{0.5}$ system where x = 0.5, it is valid: $V_{M,C}(x) = 0.5xV_{M,PbO} + 0.5(1 - x)V_{M,Bi2O3} + 0.5V_{M,\ B2O3} - 0.25x\gamma_I - 0.25(1-x)\gamma_{II}$. Using this relation and obtained V_{Mi} and γ_I, γ_{II} values, the calculated molar volume values are summarized in Table 2. The agreement between experimental $V_{M,E}$ and calculated $V_{M,C}$ values supports our suggestion that only small and rather monotonous changes in the metaborate network of $(PbO)_x(Bi_2O_3)_{0.5-x}(B_2O_3)_{0.5}$ glasses proceeds with substitution of PbO by Bi_2O_3.

Table 2. The values of calculated molar volume ($V_{M,C}$, cm^3/mol), the SWAE slope ($B^{1/2}$, (eVcm)$^{-1/2}$), width of the localized states at band edges (ΔE, meV) and the calculated values of the non-linear refractive index, ($n_2 \times 10^{-11}$[esu]) for $(PbO)_x(Bi_2O_3)_{0.5-x}(B_2O_3)_{0.5}$ glasses. In parentheses, the values of relative error ($=100(V_{M,C} - V_{M,E})/V_{M,E}$) are given.

x	$V_{M,C}$	$B^{1/2}$	ΔE	$\gamma \times 10^{-4}$	$n_2 \times 10^{-11}$
0.1	34.88 (-2.43)	680	122	5.91	0.93
0.2	32.24 (-2.85)	523	218	5.77	0.91
0.3	29.58 (-3.12)	490	251	5.61	0.78
0.4	26.92 (-3.55)	435	320	5.35	0.73

4.2 Short wavelength absorption edge and non-linear refractive index

From the results summarized in Table 1, it is evident that the optical gap values decrease with substitution of PbO by Bi_2O_3 while the slope ($B^{1/2}$) of the SWAE

increases. Similar behaviour of the optical gap was observed for some other PbO - Bi_2O_3 - B_2O_3 glasses [12]. In our case we suppose the substitution of PbO by Bi_2O_3 means that the density of heavy metal atoms increases, which for practically equal Pb - O and Bi - O bond energy and bond distance, see 4.1., should lead to a broadening of the valence band and hence, the optical gap is narrowing. Simultaneously, an increase in Bi_2O_3 content means that the number of non-bridging oxygens could increase because a rough estimation of the ratio of Bi^{3+} and Pb^{2+} cations polarisability, equal to the square of ionic charge = 9/4, indicates that the electronic shell of the oxygen ion could be more affected by highly polarising Bi^{3+} ion. Hence, an enhancement in the number of NBO is possible which also leads to a narrowing in the optical gap. Within Davis and Mott model [6], the slope of SWAE could be expressed by eqn:

$$B = (4\pi/nc)\sigma_{min}/\Delta E , \quad (1)$$

where n, c, σ_{min} and ΔE are the refractive index, the light velocity, the minimum metallic conductivity and the width of localized states at the band edges, respectively [16].

Using our experimental B and n values, and assuming $\sigma_{min} \approx 300\ \Omega^{-1}cm^{-1}$ we calculated ΔE values, see Table 2. The decrease in ΔE values with a decrease in PbO content indicates that the width of localized states at the band edges decreases and hence, some network ordering proceeds. This finding agrees with our Raman spectroscopy results indicating that the substitution of Bi_2O_3 by PbO results to an increase in the structural order of borate network.

The optical gap of various glasses and optical crystals is known to be related the non-linear refractive index (n_2) see e.g. [30, 31]. Recently, we suggested very simple relation between E_g and n_2 in the form [32]:

$$n_2[esu] \approx 1.26\times10^{-9}[esu(eV)^4]/ E_g^4. \quad (2)$$

Using this relation calculated n_2 values are summarized in Table 2. In Ref. [12] for metaborate $(PbO)_{0.25}(Bi_2O_3)_{0.25}(B_2O_3)_{0.5}$ glass experimental value of the third order non-linear susceptibility ($\chi^{(3)}$) was found 5.8×10^{-13} [esu] which using $n_2 = 12\pi\chi^{(3)}/n$, where n = 1.94 is the linear refractive index [12], gives $n_2 = 1.12\times10^{-11}$ [esu] the value close to our n_2 values we calculated from rel. (2).

5. Conclusions

The Raman spectra of studied $(PbO)_x(Bi_2O_3)_{0.5-x}(B_2O_3)_{0.5}$ metaborate glasses indicate that substitution of PbO by Bi_2O_3 leads to rather subtle changes in the Raman scattering namely:

1) In the region of heavy metal atoms activity the Raman scattering intensity increases mainly because the density of heavy metal atom – oxygen bonds increases.

2) Narrowing of the Raman feature at around 920 cm^{-1} for x = 0.1 indicates an increase of order associated with $BØ_4^-$ tetrahedra.

The optical gap decreases with the substitution of PbO by Bi_2O_3 and simultaneously also the width of localized states at the band edges decreases. The values of the non-linear refractive index have been estimated from the optical gap values in good agreement with n_2 value of similar metaborate glass (x = 0.25) reported in the literature.

Acknowledgements

This work was supported by the project VZ 0021627501. L.T. acknowledges support from the project AVOZ 40500505.

References

[1] J.C. Lapp, W. H. Dumbaugh, M. L. Powley. Riv. Staz. Sper. Vetro **1,** 91 (1989).
[2] S. Tanabe, K. Hirao, N. Soga, J. Non-Cryst. Solids **122,** 79 (1997).
[3] Y.G. Choi, J. Heo, J. Non-Cryst. Solids **217**, 199 (1997).
[4] G. Sharma, K.S. Thind, Monika, H.Singh, Manupriya, L. Gerward, phys. stat. sol. (a), **204**(2), 591 (2007).
[5] K. Kotkova, H. Ticha, L.Tichy, J. Raman Spectrosc. (2008), DOI: 10.1002/jrs.1969.
[6] E. A. Davis, N. F. Mott, Philos. Mag. **22**, 903 (1970).
[7] F. H. El-Batal, M. Azooz, F. M. Ezz-Eldin, Phys.Chem. Glasses **43,** 260 (2002).
[8] Y. Cheng, H. Xiao, W. Guo, W. Guo, Thermochimica Acta **444**, 173 (2006).
[9] T. Watanabe, K. Muratsubaki, Y. Benino, H. Saitoh, T. Komatsu, J. Mat. Sci. **36,** 2427 (2001).
[10] Z. Pan, S. H. Morgan, B. H. Long, J. Non- Cryst. Solids **185,** 127 (1995).
[11] I. Oprea, Opt. Mater. **26,** 235 (2007).
[12] K. Terashima, T. H. Shimoto, T. Yoko, Phys. Chem. Glasses **38,** 211 (1997).
[13] S. E. Van Kirk, S. W. Martin, J. Amer. Ceram. Soc. **75,** 1028 (1992).
[14] J. C. Lapp, W. H. Dumbaugh, M. L. Powley, Proc.SPIE Int.Soc.Opt.Engrs. **1327,** 162 (1990).
[15] M. E. Lines, J. Non-Cryst. Solids **89,** 141 (1987).
[16] L. Baia, R. Stefan, J. Popp, S. Simon, W. Kiefer, J. Non-Cryst. Solids **324,** 109 (2003).
[17] A. E. Miller, K. Nassau, K. B. Lyons, M. E Lines, J. Non-Cryst. Solids **99,** 289 (1988).
[18] G. D. Chryssikos, M. S. Bitsis, J. A. Kapoutsis, E. I. Kamitsos, J. Non-Cryst. Solids **217,** 278 (1997).
[19] S. D. Ross, Inorganic Infrared and Raman Spectra, McGraw-Hill, London, 1972, p. 202.
[20] M. Volf, Chemical Approach to Glass, Amsterdam, p. 129 (1984).

[21] W. H. Dumbaugh, J. C. Lapp, J. Amer. Ceram. Soc. **75,** 2315 (1992).
[22] M. E. Lines, A. E. Miller, K. Nassau, K. B. Lyons, J. Non-Cryst. Solids **89,** 163 (1987).
[23] A. M. Zahra, C. Y. Zahra, B. Piriou, J. Non- Cryst. Solids **155,** 45 (1993).
[24] L. Baia, R. Stefan, W. Kiefer, S. Simon, J. Raman Spectrosc. **36,** 262 (2005).
[25] A. A. Kharlamov, R. M. Almeida, J. Heo, J. Non-Cryst. Solids **202,** 233 (1996).
[26] G. D. Chryssikos, M. S. Bitsis, J. A. Kapoutsis, E. I. Kamitsos, J. Non-Cryst. Solids **217,** 278 (1997).
[27] W. L. Konijnendijk, W. L. Stevels, J. Non-Cryst. Solids **18,** 307 (1975).
[28] E. I. Kamitsos, M. A. Karakassides, G. D. Chryssikos, Phys. Chem. Glasses **30,** 229 (1989).
[29] O. V. Mazurin, M. V. Streltsina, T. P. Shvaiko-Shvaikovskaya, in Handbook of Glass Data, Part B, Single – Component and Binary Non-Silicate Oxide Glasses, Elsevier, 1985.
[30] M. Sheik- Bahae, D. J. Hagan, E. W. Stryland, Phys. Rev. Letters **65**, 96 (1990).
[31] T. Hashimoto, T. Yoko, Appl. Opt. **34,** 2941 (1995).
[32] H. Ticha, L. Tichy, J. Optoelectron. Adv. Mater. **4,** 381 (2002).

*Corresponding author: Helena.Ticha@upce.cz